

Supplement of Wind Energ. Sci., 5, 745–758, 2020
<https://doi.org/10.5194/wes-5-745-2020-supplement>
© Author(s) 2020. This work is distributed under
the Creative Commons Attribution 4.0 License.



Supplement of

Experimental investigation of aerodynamic characteristics of bat carcasses after collision with a wind turbine

Shivendra Prakash and Corey D. Markfort

Correspondence to: Corey D. Markfort (corey-markfort@uiowa.edu)

The copyright of individual parts of the supplement might differ from the CC BY 4.0 License.

This supplementary information document presents the detailed procedure and results of Gaussian distribution fitting to pixel coordinate and intensity measurements of Hoary bat drop #1 experiment images, to determine the carcass centroid (Section S1). The document describes the steps of the proposed methodology to determine carcass drag coefficient (C_d), by optimized coarsening window (Δt_c) and initial drop height (z_0) (Section S2). It also presents the multivariable optimization procedure illustrated in figures showing the filtering window (Δt) vs. root mean square error in velocity ($RMSE_w$) and $RMSE_w$ heatmap in $z_0 - C_d$ plane, for each of the three bat species (Section S3).

S1. Determination of position from images using recommended method in Mann et al. (1999)

The proposed methodology determines the position on images with the precision of 0.10 pixels – 0.02 pixels, by fitting a Gaussian function to the particle pixel grey intensity. We show here results from the recommended procedure as applied to the position measurements of drop #1 of Hoary bat carcass experiment. The carcass position measurements from the recommended method is compared with the earlier measurements obtained from mean of carcass top and bottom pixel coordinates. Figure S1 shows the snapshot of the greyscale image at $t = 0.420$ s during drop #1 of Hoary bat carcass. The image has been cropped to focus on the region around the carcass image. The greyscale intensity between 0 – 255 is described at each pixel coordinate encompassed in Fig. S1. The rectangular area enclosing the carcass and surrounding interrogation region covers 15 pixels (horizontally) and 13 pixels (vertically). The carcass image occupies eight pixels or 57 mm (1 pixel = 7.10 mm). The coordinates of each pixel in horizontal (x_{pixel}) and vertical (z_{pixel}) direction and pixel intensities (I_{pixel}) displayed in Fig. S1 were recorded. The pixel intensities were summed over all x_{pixels} to yield the total pixel intensity (I_{Total}) as a function of z_{pixel} . Table S1 shows I_{Total} at each z_{pixel} of the rectangular area in Fig. S1.

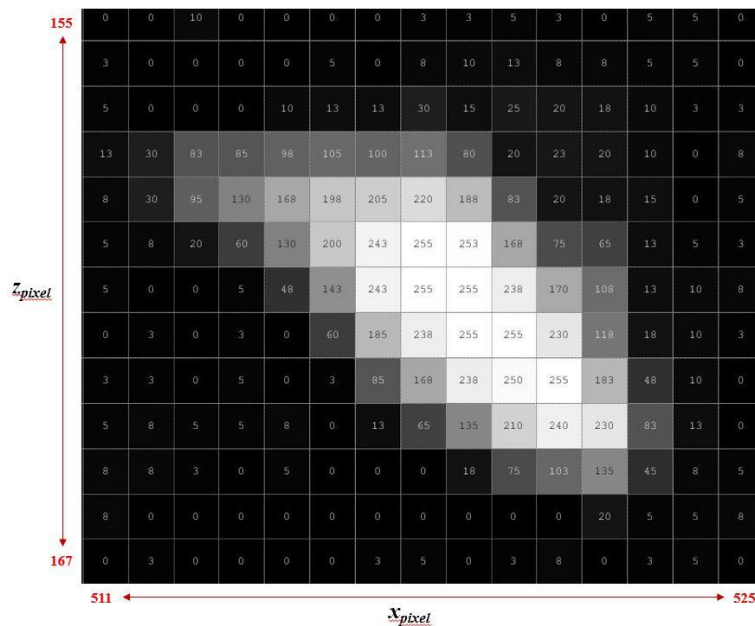


Fig. S1: Selected grey area pixels around carcass at $t = 0.420$ s

Table S1: I_{Total} at a given z_{pixel}

z_{pixel}	I_{Total}
155	34
156	65
157	165
158	780
159	1383
160	1503
161	1501
162	1378
163	1251
164	1020
165	413
166	46
167	30

Figure S2 shows z_{pixel} vs. I_{Total} plot (red dots) for the measurements in Table S1. The centroid of greyscale intensity in Table S1 was computed by averaging each z_{pixel} based on its I_{Total} value (Eq. (S1)) and was found to be 161.123. The carcass centroid from top and bottom pixel coordinate was estimated as 160. This procedure was repeated for next four consecutive images and carcass centroid was calculated for each of the image frames.

$$z_{c,new} = \frac{\sum I_{pixel} z_{pixel}}{\sum I_{pixel}} \quad (S1)$$

Table S2 below displays the comparison of z_c from two methods, i.e., mean top and bottom method (2nd column) and center of intensity method (3rd column) for the selected greyscale frames. It is evident from the table that maximum z_c difference is of the order of approximately 1 pixel from the two methods.

Table S2: Comparison of z_c

t (s)	z_c (Mean top and bottom method) (m)	z_c (Center of Intensity method, S1) (m)	$ \Delta z_c $ (mm)
0.420	5.928	5.919	9
0.424	5.903	5.900	3
0.428	5.879	5.876	3
0.432	5.857	5.853	4
0.436	5.836	5.830	6

Mann et al. (1999) proposed fitting particle images with a Gaussian shape function to determine the position from the images. A similar procedure was applied to the measured distribution shown in Fig. S2 to compute the centroid of the distribution, z_c . The Gaussian distribution expressed by Eq. (S2) was fitted to z_{pixel} vs. I_{Total} data in Table S1 to find the best estimate of carcass centroid, z_c , at $t = 0.420$ s. Figure S2 shows the Gaussian distribution (black line) fitted to z_{pixel} vs. I_{Total} measurements to give $z_c = 160.988$.

$$I_{Total} = \frac{1}{\sigma_z \sqrt{2\pi}} e^{-\frac{1}{2} \left(\frac{z_{pixel} - z_c}{\sigma_z} \right)^2} \quad (S2)$$

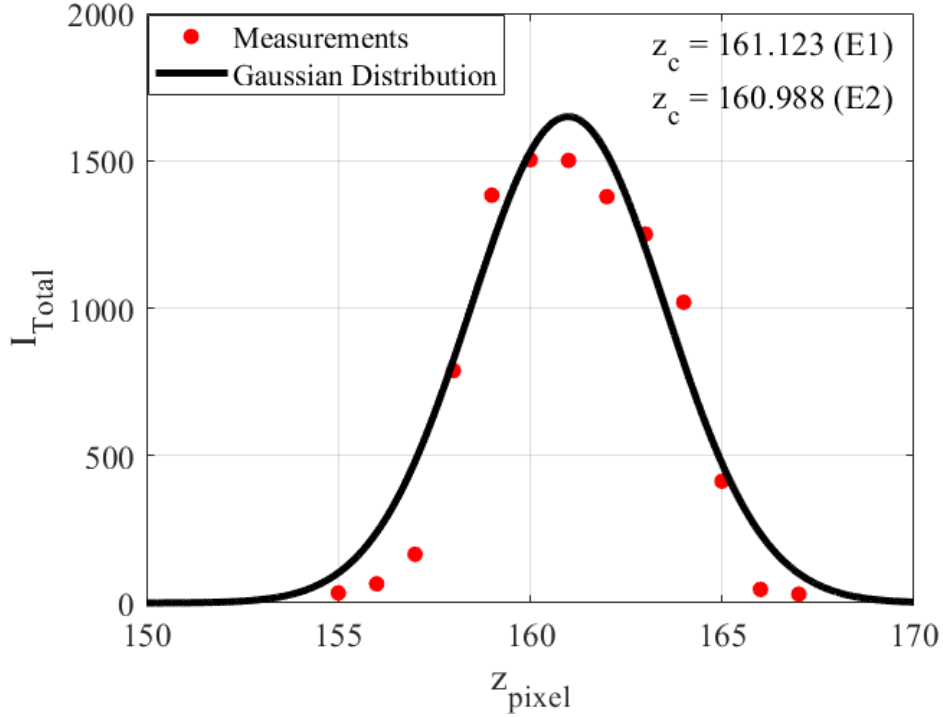


Fig. S2: Gaussian distribution fitted to z_{pixel} vs. I_{Total} measurements

The Gaussian distribution was fitted to z_{pixel} vs. I_{Total} measurements of the next consecutive images to determine the respective centroids. Table S3 shows the comparison of the carcass centroid estimated using top and bottom pixels (2nd column) and by fitting Gaussian distribution (3rd column) to z_{pixel} vs. I_{Total} measurements. Again, we notice from Table S3 that the difference in the z_c estimates from the two approaches are of the order of 1 pixel.

Table S3: Comparison of z_c

t (s)	z_c (Mean top and bottom method) (m)	z_c (Gaussian fitting, S2) (m)	$ \Delta z_c $ (mm)
0.420	5.928	5.920	8
0.424	5.903	5.898	5
0.428	5.879	5.875	4
0.432	5.857	5.852	5
0.436	5.836	5.829	7

S2. Proposed multivariable optimization algorithm

1. With the assumption, $w_0 = 0$, one degree of freedom in the problem is reduced, leaving three degrees of freedom ($\Delta t_c, z_0, C_d$).
2. An array of plausible z_0 and C_d values is declared and then the ballistics model was solved for the prescribed values of z_0 and C_d . The z_0 array with m elements and C_d array with n elements results in $m \times n$ fall trajectories.
3. An array representing different resolutions, Δt , of measured velocity with p elements is defined. The measured velocity at different resolutions is fitted to $m \times n$ fall trajectories. This leads to $m \times n$ number of $z_0 - C_d$ combinations of fall trajectories fitted to p different resolutions of measured velocity.
4. For each of the $m \times n \times p$ fitting events, root mean square error in fall velocity ($RMSE_w$) at i^{th} time instant is estimated using the following formula:

$$RMSE_w = \sqrt{\frac{\sum_{i=1}^n (w_{model}(i) - w_{field}(i))^2}{n}} \quad (S3)$$

where w_{model} represents the velocity obtained from the ballistics model solution and w_{field} represents the measured velocity from high – speed imaging of carcass drop experiments. The variable n is the number of data points in velocity time series for a specific coarsening window.

5. For $m \times n$ combinations of z_0 and C_d , Δt vs. $RMSE_w$ is plotted. The range of Δt values over which $RMSE_w$ remains invariant for $z_0 - C_d$ combinations is identified. The basis of selecting Δt range of invariant $RMSE_w$ is: the relative error in successive $RMSE_w$ values being less than 10%.

$$RELError(i) = \left(\frac{RMSE_w(i+1) - RMSE_w(i)}{RMSE_w(i)} \right) \times 100 \quad (S4)$$

where $RMSE_w(i+1)$ and $RMSE_w(i)$ are the two successive values in $RMSE_w$ vector at $(i+1)^{\text{th}}$ and i^{th} time step for a specific $z_0 - C_d$ combination. $RELError(i)$ is the relative error in $RMSE_w$ at i^{th} time step.

6. For each element in Δt vector (which corresponds to invariant $RMSE_w$) representing a plausible optimum resolution of the measured velocity, the optimal z_0 and C_d is computed by defining $(RMSE_w)_{min}$ as the objective function. The temporal resolution of extracted data (0.004 s) yields serious scatter in the measured velocity which makes it impossible to find the best – fit of ballistics model to the measured velocity. For large filtering window of the measured data, the order of the ballistics model becomes equal to the number of the data points; hence giving the biased estimate of $RMSE_w$. The objective for selecting the Δt range of constant $RMSE_w$ is to find an unbiased estimator of the goodness of fit and therefore, range of Δt yielding invariant $RMSE_w$ is selected as possible candidates for determining the optimal coarsening window.
7. From step 6, a pool of initial positions (z_0) and drag coefficients (C_d) for varying resolutions of measured velocity (embedded in Δt vector corresponding to constant $(RMSE_w)_{min}$) is obtained. Out of this pool, the value of Δt , z_0

and C_d giving the global minimum $(RMSE_w)_{min}$ is selected as optimum data resolution, initial position, and carcass drag coefficient, respectively.

8. To test the accuracy of the optimum Δt_c , z_0 and C_d , the analytical solution of the ballistics model from optimized z_0 and C_d estimates is compared with the measured position and velocity at the optimum resolution (Δt_c).

S3. Optimized drag coefficient estimates

The optimization algorithm steps described in section S2 were applied to the carcass fall velocity data to determine the carcass drag coefficient of the three discovered species. Following are the results of the optimization process:

S3.1 Hoary bat

For carcass drop experiment, z_0 was defined between 7.40 m and 7.80 m at an increment of 0.01 m whereas C_d array was selected between 0.50 and 1 with differential C_d being 0.01. In this manner, there are overall 41×51 $z_0 - C_d$ combinations leading to equal number of carcass fall trajectories. The Δt array was chosen from 0.004 s to 0.512 s at an increment of 0.004 s. This declaration of $z_0 - C_d - \Delta t$ culminated in $41 \times 51 \times 128$ ballistics model fitting events to the measured velocity. For each of these cases, $RMSE_w$ was calculated through difference in the modelled velocity and measured velocity values.

Three – point centered moving average of $RMSE_w$ vector was computed and plotted with Δt (for all $z_0 - C_d$ combinations) in order to identify Δt range of invariant $RMSE_w$ on the basis of $RELErr$ < 10%. Figure S3 (a) demonstrates the Δt vs. $RMSE_w$ plot, for the lower ($z_0 = 7.40$ m and $C_d = 0.50$) and upper ($z_0 = 7.80$ m and $C_d = 1$) bounds of z_0 and C_d array respectively. The Δt range corresponding to invariant $RMSE_w$, was found to be between 0.060 and 0.104 s (region between the two vertical arrows in Fig. S3 (a)). Optimum z_0 and C_d were calculated by minimizing $RMSE_w$ for each element in Δt vector corresponding to invariant $RMSE_w$. Ultimately, the global minimum $(RMSE_w)_{min}$ was selected as a criterion for Δt_c , z_0 and C_d , in highlighted spectrum of Δt giving invariant $RMSE_w$. Fig. S3 (b) shows the plot of $RMSE_w$ in the $z_0 - C_d$ plane at an optimal resolution of $\Delta t_c = 0.104$ s, in highlighted domain of Δt vector. The red dot in the heatmap displays the optimum $z_0 = 7.58$ m and $C_d = 0.70$ yielding global minimum $(RMSE_w)_{min}$ of 0.067 m/s.

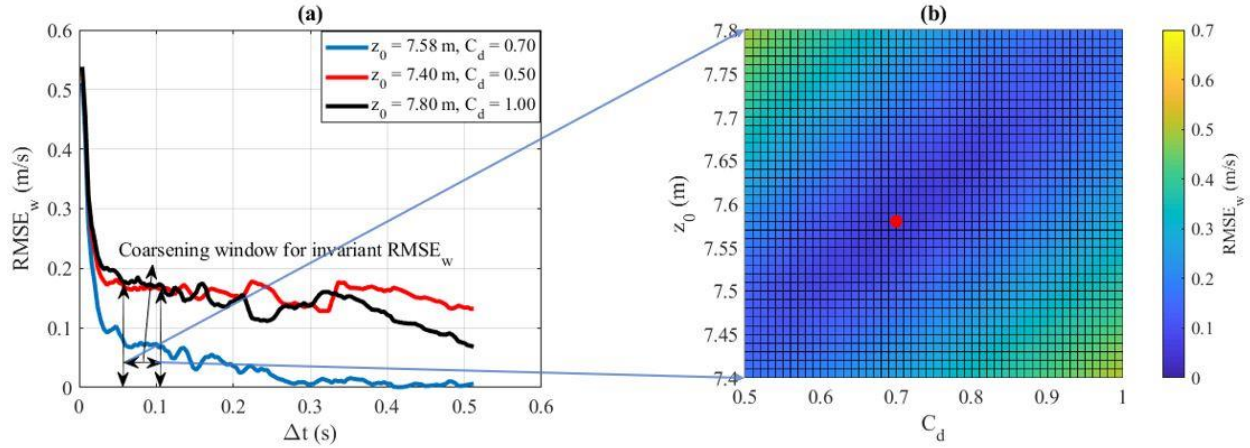


Fig. S3: (a) Δt vs. $RMSE_w$ plot; (b) $RMSE_w$ heatmap in $z_0 - C_d$ plane (Hoary bat)

S3.2 Eastern Red bat

For analyzing Eastern Red bat, z_0 , C_d and Δt were defined in the same manner as with the Hoary bat. This declaration of $z_0 - C_d - \Delta t$ culminated in $41 \times 51 \times 128$ ballistic model fitting events to the measured velocity. For each of these cases, $RMSE_w$ was calculated through difference in the modelled velocity and measured velocity values. Again, three – point centered moving average of $RMSE_w$ vector was computed and plotted with Δt (for all $z_0 - C_d$ combinations) in order to identify Δt range of invariant $RMSE_w$ on the basis of $RELError < 10\%$.

Figure S4 (a) demonstrates the Δt vs. $RMSE_w$ plot, for the lower and upper bounds of z_0 and C_d array respectively. The spectrum of Δt corresponding to invariant $RMSE_w$ was found to be between 0.080 s and 0.152 s (region between the two vertical arrows in Fig. S4 (a)). For each element in the above – mentioned Δt range of invariant $RMSE_w$, the optimum z_0 and C_d were calculated by minimizing $RMSE_w$ and then from this pool of $(RMSE_w)_{min}$, global minimum $(RMSE_w)_{min}$ was selected as the criteria to identify Δt_c , optimized z_0 and C_d for that specific carcass drop experiment. Figure S4 (b) shows the plot of $RMSE_w$ in $z_0 - C_d$ plane, at an optimum filtering of $\Delta t_c = 0.152$ s, in the marked range of Δt vector. The optimized z_0 (7.63 m) and C_d (0.80) corresponding to the global minimum $(RMSE_w)_{min}$ of 0.044 m/s, is highlighted by red dot in Fig. S4 (b).

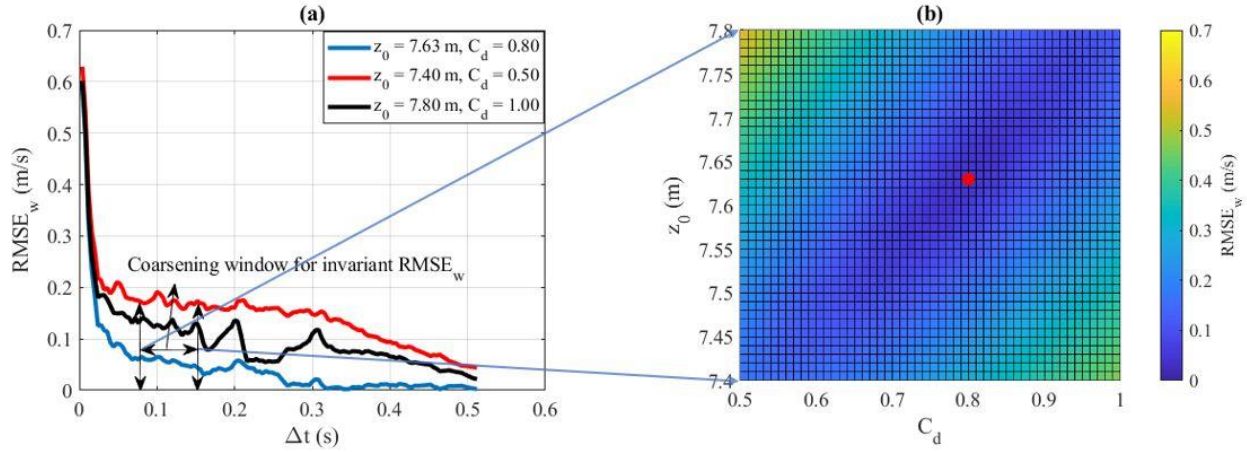


Fig. S4: (a) Δt vs. $RMSE_w$ plot; (b) $RMSE_w$ heatmap in $z_0 - C_d$ plane (Eastern Red bat)

S3.3 Evening Bat

For Evening bat, z_0 array was declared between 6.90 m and 7.70 m with differential z_0 being 0.01 m whereas C_d vector was defined between 0.90 and 1.20 at an increment of 0.01. Δt array was kept the same as it was with Eastern Red bat and Hoary bat. This declaration generated overall $81 \times 31 \times 128$ ballistics model fitting events to the different filtering windows of measured velocity.

Figure S5 (a) shows the Δt vs. $RMSE_w$ (moving averaged) plot, for the lower and upper bounds of z_0 and C_d array respectively. Δt range corresponding to invariant $RMSE_w$ was established between 0.132 s and 0.144 s (region between vertical arrows in Fig. S5 (a)) and global minimum $(RMSE_w)_{min}$ was selected as a criterion for Δt_c , optimized z_0 and C_d , within marked range of Δt . The red dot in Fig. S5 (b) represents optimal values of $z_0 = 7.20$ m and $C_d = 1.01$ with global minimum $(RMSE_w)_{min}$ of 0.078 m/s for $\Delta t_c = 0.144$ s.

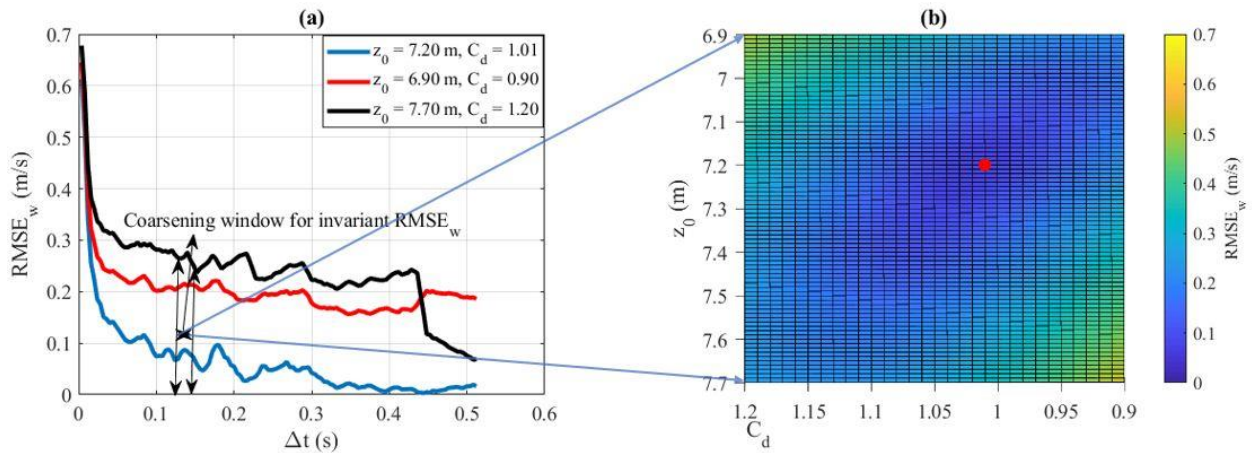


Fig. S5: (a) Δt vs. $RMSE_w$ plot; (b) $RMSE_w$ heatmap in $z_0 - C_d$ plane (Evening bat)